

Continual Learning of Semantic Segmentation using Complementary 2D-3D Data Representations

Jonas Frey¹, Hermann Blum², Francesco Milano², Roland Siegwart², Cesar Cadena²

Abstract—Semantic segmentation networks are usually pre-trained and not updated during deployment. As a consequence, misclassifications commonly occur if the distribution of the training data deviates from the one encountered during the robot’s operation. We propose to mitigate this problem by adapting the neural network to the robot’s environment during deployment, without any need for external supervision. Leveraging complementary data representations, we generate a supervision signal, by probabilistically accumulating consecutive 2D semantic predictions in a volumetric 3D map. We then retrain the network on renderings of the accumulated semantic map, effectively resolving ambiguities and enforcing multi-view consistency through the 3D representation. To preserve the previously-learned knowledge while performing network adaptation, we employ a continual learning strategy based on experience replay. Through extensive experimental evaluation, we show successful adaptation to real-world indoor scenes both on the ScanNet dataset and on in-house data recorded with an RGB-D sensor. Our method increases the segmentation performance on average by 11.8% compared to the fixed pre-trained neural network, while effectively retaining knowledge from the pre-training dataset.

I. INTRODUCTION

Robotic perception tasks such as semantic segmentation or object detection rely on large-scale neural networks, which require gathering and annotating large datasets to be trained. This tedious process is costly, time-intensive, and error-prone. Furthermore, a dataset captured at a fixed point in time cannot fully cover every possible data point in the future for complex tasks in unknown environments. This leads to the common problem of a distribution mismatch between the available labeled dataset (source domain) and the actual data of interest (target domain) encountered in a robot’s mission. In semantic segmentation, such domain gaps commonly cause misclassification of unknown categories and wrong labeling of small semantic details in favor of the dominant neighboring semantic class [1]. While these limitations call for the need of performing network adaptation in new environments, a straightforward adaptation is hindered by the lack of a ground-truth supervision signal during deployment.

Fortunately, mobile robots can usually observe the same area of their deployment environment from different viewpoints, which thus potentially provides the means to resolve semantic ambiguities. Standard approaches for semantic segmentation operate on a per-frame basis, producing a prediction for each image separately. Small, occluded or partially observed objects may therefore be misclassified due to the lack of sufficient context, but may be correctly classified



Fig. 1: Comparison of semantic segmentation performance of in-house recorded conference room scene. From top to bottom: Pre-trained network predictions (1-Pred), rendered pseudo-labels leveraging multi-view consistency (1-Pseudo), our adapted network predictions after training on 1-Pseudo with a continual learning strategy (2-Pred), ground truth annotated by us.

in consecutive frames with different viewpoints. While a number of works integrate semantic predictions into a global 3D representation to achieve more consistent labeling of the scene [2], [3], [4], none of these approaches leverages the view consistency to adapt the semantic segmentation network, which in their experiments is only trained once before deployment and not updated during the mission. As illustrated in Figure 1, this work instead proposes to explicitly leverage multi-view consistency both to increase the robustness of the semantic labels and to adapt the network to a new environment. To this extent, we accumulate individual 2D semantic predictions into a 3D map and generate a new training signal for the network by reprojecting the fused semantic information back into 2D pseudo-labels. To the best of our knowledge, we are the first to propose adapting a neural network according to a supervision signal generated by explicitly transforming network predictions between 2D and 3D. Through extensive experimental evaluation, we show that the multi-view consistency enforced by this supervision signal allows the network to reliably increase its accuracy with respect to a fixed network.

Naïve adaptation of the network to the generated supervision signal can however cause forgetting of previously-acquired knowledge. This is undesirable for mobile robots,

¹ Robotic Systems Lab, ETH Zurich, Switzerland

² Autonomous Systems Lab, ETH Zurich, Switzerland

which have to frequently change operating environments, but can possibly return to previously encountered scenes. This problem relates to the field of continual learning, which studies how previous knowledge can be preserved while new one is integrated into a neural network. To achieve the adaptation of the network to the current environment while counteracting forgetting, we adopt an experience replay continual learning strategy [5], regularizing the adaptation to the pseudo-labels with stored samples from the pre-training dataset. Contrary to the other methods that explore semantic segmentation in a continual learning setting, our approach is suited for online deployment, exploits a 3D representation to enforce multi-view consistency, and only requires an RGB-D sensor and the associated camera poses.

We evaluate our method on the indoor, real-world ScanNet [6] dataset, showing a remarkable increase of the semantic segmentation performance on average by 11.8% relative to the static network. Additionally, we provide qualitative deployment experiments with a handheld RGB-D sensor.

To summarize, our main contributions are the following:

- 1) We propose a method to leverage complementary data representations to generate accurate pseudo-labels;
- 2) We employ the generated pseudo-labels to adapt a semantic segmentation network using continual learning during a robotic mission;
- 3) We present quantitative evaluation on both a real-world dataset and in real-world experiments using an RGB-D sensor, showing consistent improvement of the prediction accuracy of the adapted network.

II. RELATED WORK

A number of previous works have proposed methods that fuse information from different viewpoints to achieve better semantic understanding of a scene. SemanticFusion [7] leverages a semantic segmentation network and a SLAM system to create a surfel-based representation of the scene, which probabilistically accumulates semantic information.

Kimera [3] uses a similar approach but tracks semantics using a regular voxel grid instead of surfels. Voxblox++ [2] identifies individual object instances and organizes them in a volumetric object-centric map. More recently, [8] proposed to augment a 3D representation of the environment with hierarchical scene graphs, which encode relationships between elements. All the above methods, however, rely on a fixed network which is assumed to be accurate and not updated with the semantic information collected in the generated map. On the contrary, we propose a method that accumulates semantic information similarly to [3], but continually trains the neural network using the accumulated information about the current environment in an unsupervised manner. To deal with the problem of learning in the absence of full supervision, the fields of unsupervised and semi-supervised semantic segmentation leverage unlabeled data to learn representations. Approaches in this field achieve state-of-the-art performance in visual representation learning [9], but are mainly studied as offline pre-training mechanisms [10]. Particularly relevant for our approach is also the recent work

in representation learning proposed by [11], which highlights the benefit of leveraging the view consistency enforced in 3D as a prior for 2D tasks involving semantics. However, while this work focuses on offline pre-training of network features, we explicitly integrate predictions in 3D and tackle an online setting with adaptation of the network to new data.

The problem of integrating new knowledge into a network is a core research question in the field of continual learning [12], where the main focus is on preventing the accuracy on previously seen data from decreasing significantly when training on a new data distribution, a commonly-observed phenomenon referred to as catastrophic forgetting [13]. Among the different strategies proposed to address this issue, experience replay has proven to be particularly effective [14], [5], [15], [16], often outperforming approaches based on more complex designs [17], [18]. In experience replay, a subset of previously learned samples is stored and used to regularize the training procedure. Despite its relevance for real-world settings, where non-stationary data distributions are common, little research is conducted to address robotic settings within the continual learning field. The sparse existing literature evaluates on a small scale or unrealistic problem sets [15], [16], [19], and mainly focuses on classification tasks [20], [21], [19].

A limited number of works has explored semantic segmentation in continual learning [22], [23], [24], [25], [26]. However, these approaches are not designed for application in an online scenario, tackle segmentation purely in 2D on a per-frame basis, and rely on the availability of ground-truth supervision. On the contrary, we focus on the setting of online deployment where no ground-truth labels are available, and exploit multi-view consistency across frames, both to increase the robustness of the segmentation and to generate a learning signal for adaptation. Recently, the authors of [27] proposed to adopt a continual learning strategy to improve the segmentation and localization capability of a construction robot in a self-supervised manner. However, their approach relies on known building meshes and a LiDAR sensor to generate pseudo-labels. Additionally, it is only evaluated on the task of binary classification into fore- and background. Our method is more versatile, as it performs multi-class semantic segmentation and does not rely on any external knowledge such as precise CAD maps or expensive sensors.

III. APPROACH

Our proposed method consists of two main components:

- 1.) The *Pseudo-Label Generation* (Sec. III-A) probabilistically accumulates semantic information in a 3D voxel-based map and generates pseudo-labels using ray tracing.
- 2.) The *Continual Learning* (Sec. III-B) component adapts the parameters of the neural network and receives as input the generated pseudo-labels with the corresponding camera images. It is implemented using an experience replay continual-learning strategy and minimizing the cross-entropy between the generated pseudo-labels and the network predictions.

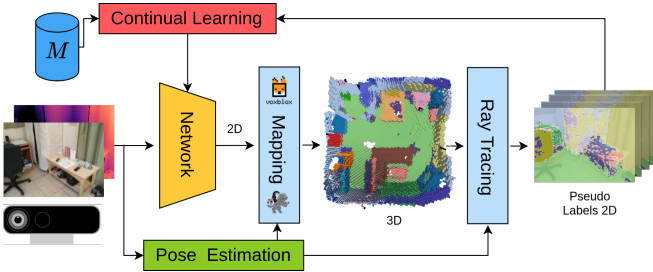


Fig. 2: Overview: An RGB-D camera provides depth and image data to a segmentation network (yellow) and pose estimation module (green). Individual 2D semantic estimates are accumulated in a 3D voxel map. The generated map is ray traced to create 2D pseudo-labels. The pseudo-labels are used to adapt the network using a continual learning strategy (red), which can access previously stored samples in a memory buffer (dark blue) to regularize the training.

A. Pseudo-Label Generation

A pre-trained semantic segmentation network f_θ predicts initial semantic estimates Y_n^{pred} from a provided video sequence consisting of individual key frames I_n , where n denotes the index in the sequence of length N . We create a dense semantic map of the robot’s environment using a voxel-based truncated signed distance function (TSDF). In addition to the TSDF volume, a semantic voxel volume stores the probability of each voxel belonging to a semantic class. The camera extrinsics H_n , and depth map D_n are used to integrate the predicted semantics Y_n^{pred} into both volumes. The TSDF is calculated following [28]. For each voxel close to the TSDF surface, the semantic label probability is updated following recursive Bayesian estimation [3]. The mapping procedure is performed for each camera trajectory within a scene individually. After integration of all N measurements, Marching Cubes [29] is used to estimate a high-resolution mesh. We ray trace the mesh for each camera pose H_n to determine for each pixel in the camera plane the first intersection of the corresponding ray with the mesh. Each of the resulting 3D locations is then used to index the semantic voxel volume in $O(1)$ time to retrieve the semantic label probabilities for the associated pixel. We refer to the resulting re-projected semantic segmentation label as Y_n^{pseudo} as *pseudo-label*. The pseudo-labels aggregate information from multiple viewpoints and enforces multi-view consistency. At the same time, gathering information from multiple viewpoints allows filtering out semantic segmentation errors induced by bad lighting, motion blur, and outlier predictions in individual frames. This allows us to generate a learning signal of higher accuracy that can be used to adapt the network in the absence of ground-truth supervision. We exploit the learning signal to adapt the pre-trained network’s parameters θ (Sec. III-B). Exact implementation details are discussed in Section IV.

B. Continual Learning

While it would be possible to directly replace the single-frame prediction of the segmentation network with the

pseudo-labels, we instead use the pseudo-labels to train the neural network and adapt it to the scene. This has two reasons. First, the accuracy gain of the pseudo-labels cannot be transferred to a different environment, since the map is bound to the geometry of the scene. The (adapted) network however has the ability to transfer the gained knowledge to any future frame from any environment. Second, the pseudo-labels themselves require sufficient prediction accuracy of the network, while the network training has the potential to filter out undesirable artifacts from the voxel rendering.

For training, we one-hot encode the pseudo-labels according to the most likely class per pixel. This experimentally outperformed the probabilistic pseudo-labels and reduces storage and computation needed. To update the model parameters θ we use an experience replay strategy. For this, a small subset of N_M randomly selected samples of pre-training dataset is stored in a memory buffer M , which can be accessed to *replay* samples (i.e., feed them again to the network) when adapting the parameters θ to the current scene. The standard cross-entropy loss function is used for both the new samples annotated with the pseudo-labels and the replayed samples with ground-truth annotations. We use stochastic gradient descent (SGD) [30] to optimize the cross-entropy loss function. We can explicitly distinguish between the loss induced by samples stored in the memory buffer and the pseudo-labels in the SGD update:

$$l_{\text{total}} = \sum_{i=1}^{n_{\text{pseudo}}} l_{\text{CE}}(f_\theta(x_i), y_i) + \sum_{j=1}^{n_{\text{rep}}} l_{\text{CE}}(f_\theta(x_j), y_j) \quad (1)$$

$$\theta_{t+1} = \theta_t - \frac{\mu}{n_{\text{pseudo}} + n_{\text{rep}}} \frac{d}{d\theta} l_{\text{total}}, \quad (2)$$

where n_{rep} and n_{pseudo} denote the number of replayed and pseudo-labels samples respectively. The learning rate is denoted by μ and l_{CE} is the cross-entropy loss function.

On one side, minimizing the loss of the replayed samples motivates preservation of previously learned information: the diversity of the samples in the memory buffer favors generalization and mitigates overfitting to the small pseudo-label dataset. On the other side, the loss of the pseudo-labels encourages the learning of new knowledge. Additionally, since the samples in the memory buffer are annotated with ground-truth labels, common patterns of the ground-truth annotations may be transferred to the pseudo-labeled samples and act as a regularization mechanism. Finally, storing a subset of N_M samples significantly reduces the memory needed with respect to the full pre-training dataset size N_{pre} . The network training routine is elaborated in Section IV.

IV. IMPLEMENTATION DETAILS

A. Network and Dataset

We use Fast-SCNN [31] as a semantic segmentation network. During inference it runs at over 250 fps using a resolution of 320×640 pixels with 1.1 M parameters. For quantitative evaluation, we use the ScanNet [6] dataset. It consists of 1513 Microsoft Kinect camera trajectories recorded at 30 fps within 707 distinct indoor spaces. For

each scan, the dataset provides a dense 3D map, which is manually annotated with NYU40 classes [32] and per-frame labels generated by 2D re-projection. The pre-training dataset consists of every 100th frame of scene 11-707 resulting in ~ 25 k frames. From this we use 20 k frames for the actual pre-training and 5 k for testing the performance on the pre-training dataset. All scans recorded in scenes 1-5 are used to evaluate the adaptation performance of our proposed method. For each scene, up to 3 separate video sequences are provided in the dataset. We chain these sequences into a single long sequence per scene, from which the first 80% of the frames are used for pseudo-label generation and continually training the network. The final 20% of the frames are only used for testing the adaptation performance. Despite the strict training-test split, the same objects may be observed within the same scene in both datasets. We stress that the created benchmark mimics a real robotic scenario, in which a large dataset of annotated data is commonly available, but adaptation during a mission has to be performed in an unsupervised manner.

B. Network Pre-Training

We train the network on the pre-training dataset using Adam [33] with a batch size of 8. The starting learning rate is set to 10^{-3} and polynomially decayed over 150 epochs to 10^{-6} with a rate of 0.9. We stop the training procedure early after 65 epochs ($\sim 200,000$ optimization steps) given convergence on a test set. During training, we apply standard data augmentation, including color jitter, horizontal flipping, and random cropping.

C. Pseudo-Label Generation

To construct the semantic map, we use Kimera Semantics [3], which builds on VoxBlox [28], a mapping framework based on voxel grids. We set the voxel resolution to 3 cm, which we found to provide a good balance between level of semantic detail captured and computational efficiency. Kimera Semantics tracks the full posterior probability for all 40 NYU40 labels per voxel. Integration of a single measurement into the TSDF and semantic volume on a Ryzen 5900X CPU takes 330 ms at a resolution of 320×640 . For typical room-sized scenes $10 - 20 \text{ m}^2$ the mesh produced by Marching Cubes has a size of 5 MB. The voxel volume storing the full uncompressed semantic posterior has a size of ~ 500 MB for $4.1 \text{ m} \times 3.6 \text{ m} \times 1.5 \text{ m}$ volume (Fig. 4). The high-performance CPU-based ray tracing implementation [34] infers pseudo-labels at a rate of 30 fps.

D. Continual Learning

We retrain the network on the generated pseudo-labels for a total of 50 epochs. SGD is used with a 1cycle learning rate schedule [35] and a batch size of 16 to adapt the parameters. The scheduler linearly increases the learning rate from 10^{-6} to 0.05 over the initial 5 epochs and successively decays it to 10^{-3} over the remaining 45 epochs. Starting with a slow learning rate is important to avoid strongly perturbing the model parameters within the first iterations

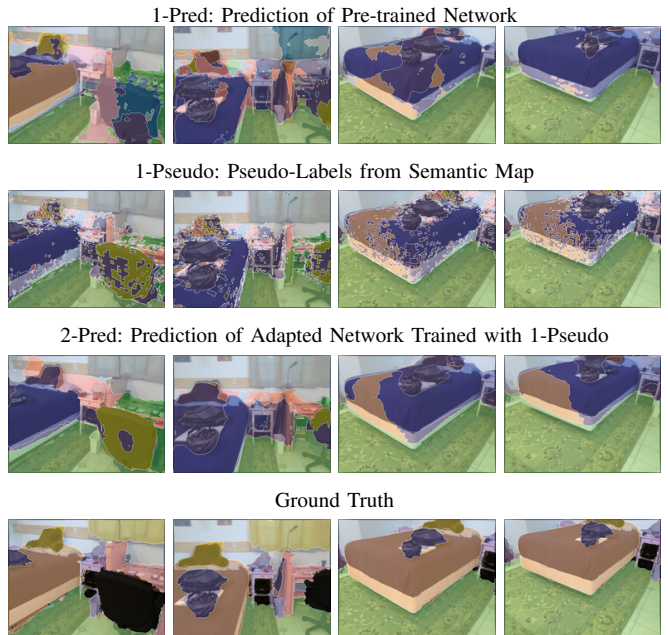


Fig. 3: Segmentation of the first scene in the ScanNet dataset, using ScanNet color coding. First row: Pre-trained network predictions (1-Pred). Second row: Generated pseudo-labels (1-Pseudo). Third row: Adapted neural network (2-Pred). Fourth row: Ground-truth labels.

of training. We empirically found that storing 10% of the pre-training dataset in the memory buffer (resulting in a memory size N_M of 2000) is capable of representing the training dataset adequately. During training the samples of each mini-batch are randomly chosen with a ratio of 4:1 from the pseudo-labels and memory buffer. We experimentally found this ratio to provide a good trade-off between integrating new knowledge and preserving the performance on the pre-training dataset. During training the same data augmentation used for pre-training is applied to the replayed and pseudo-labeled samples. We found data augmentation to be particularly beneficial for small buffer sizes, which aligns with the findings reported in [5].

V. EXPERIMENTS

In the following, we evaluate each component in the pipeline individually to measure its performance. We then test the fully operating pipeline and show experimental results for the ScanNet dataset and data recorded in the lab with a handheld RGB-D sensor.

A. Pseudo-Label Performance

To evaluate the pseudo-label generation procedure, we compare the segmentation accuracy achieved by the pre-trained neural network to the resulting pseudo-labels. An exemplar sequence of 4 frames of the first scene is illustrated in Figure 3. The pre-trained network predictions disagree for the same location over consecutive frames. The pseudo-labels include minor artifacts induced by the voxel discretization

Scene	1-Pred		1-Pseudo			2-Finetune		2-Pred (CL)	
	Gen	Adap	Adap	Δ	GT	Gen	Adap	Gen	Adap
1	43.0	60.5	70.2	9.7	94.3	36.1	71.7	37.6	71.2
2	43.0	48.5	53.7	5.2	94.9	35.7	51.6	37.2	52.9
3	43.0	30.5	38.0	7.4	88.7	34.7	36.7	36.3	36.8
4	43.0	74.6	81.6	7.0	96.0	27.3	81.3	31.8	80.6
5	43.0	40.3	44.0	3.7	88.7	24.5	41.0	32.4	42.7
AVG	43.0	50.9	57.5	6.6	92.5	31.7	56.7	35.1	56.9

TABLE I: Segmentation accuracy of pre-trained (1-Pred), fine-tuned (2-Finetune) and continual-learned (2-Pred (CL)) network, as well as pseudo-labels generated from the pre-trained network (1-Pseudo) and their upper bound (GT). We measure *adaptation* performance on the novel scenes 1-5 of the ScanNet dataset (Adap) and *generalization* performance on the pre-training test dataset (Gen).

and the ray tracing process, but are consistent over multiple iterations. Moreover, as we show in Section V-B, these artifacts are not reflected in the adapted network predictions and do not prevent the signal from being beneficial for improving the prediction accuracy.

To verify the correctness of the pseudo-label generation and set an upper bound for the pseudo-label performance, we additionally use the ground-truth segmentation to generate pseudo-labels. We report the accuracy on the test dataset for each scene and averaged over all scenes and further compute the increase in accuracy – denoted as Δ – between the input and output of the pseudo-label generation module. As shown in Table I, the pseudo-labels (1-Pseudo) generated based on the pre-trained network predictions (1-Pred) always improve the accuracy, on average by 6.6% (relative 11.8%). Since the artifacts induced by voxelization and ray tracing limit the achievable accuracy of the pseudo-labels, we also report the accuracy of the pseudo-labels generated based on the ground-truth data (GT) as an upper bound.

We illustrate the reconstructed mesh used to generate 1-Pseudo and GT-Pseudo in Figure 4. All objects can be clearly identified in the GT map. In 1-Pseudo only few misclassifications (*desk*, top right; *toilet* top left) and artifacts (*sofa* bottom middle, *bed* top middle) cannot be resolved. From this we can conclude that the pseudo-label generation process significantly improves the accuracy of the semantic segmentation and therefore is suitable as a learning signal to adapt the network.

B. Continual Learning

We compare the performance achieved by a network adapted with the naïve fine-tuning and continual learning strategy. To evaluate the broader generalization performance we measure the accuracy on the test set of the pre-training dataset and calculate the adaption performance using the accuracy on scene 1-5 of the ScanNet dataset. As shown in Table I, the experience replay strategy outperforms fine-tuning for all scenes on the pre-training dataset (+3.4%). Moreover, the average accuracy on the adaptation scene

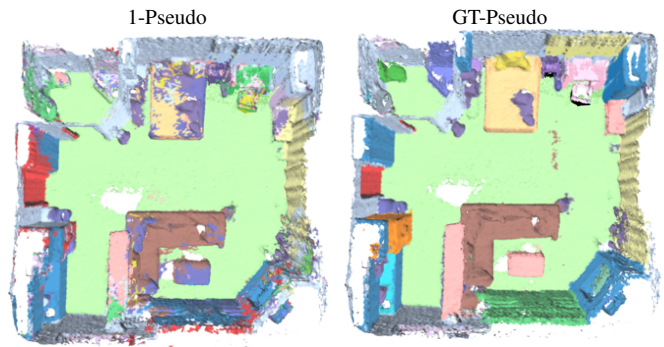


Fig. 4: Resulting mesh in the pseudo-label generation of the first ScanNet scene. Left: Pseudo-label map (1-Pseudo) generated using the pre-trained neural network. Right: Pseudo-label map (GT-Pseudo) generated using the ground-truth labels.

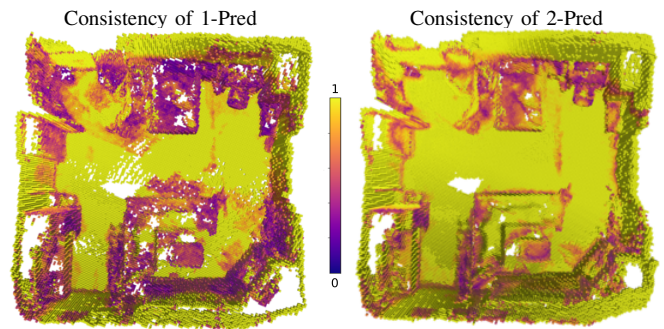


Fig. 5: Multi-view consistency measured as per-voxel confidence in the first ScanNet scene. Left: Confidence of the voxel volume when mapping the pre-trained neural network predictions (1-Pred). Right: Confidence of the voxel volume when mapping the adapted neural network prediction in the second iteration (2-Pred).

slightly increases (+0.2%). The predicted semantic segmentation of the continually-learned network for the selected key-frames of the first scene are illustrated in Figure 3. As evident in the third row, they align with the pseudo-label predictions but filter out noise and artifacts, resulting in smooth boundary regions.

We can further evaluate the multi-view consistency of the network predictions before and after adaptation. When integrating disagreeing network predictions in the same voxel, the uncertainty of the specific voxel increases. Figure 5 shows these voxel uncertainties after integrating predictions from the pre-training network (1-Pred) and the adapted, continually-learned network (2-Pred). Clearly, our adaptation procedure increases the overall certainty and therefore multi-view consistency of 2-Pred over 1-Pred.

C. Iterative Operation

The process of generating pseudo-labels and adapting the neural network using continual learning can also be performed for multiple steps within the same scene, by iteratively generating pseudo-labels and retraining the network on

Scene	1-Pred	1-Pseudo	2-Pred	2-Pseudo	3-Pred	3-Pseudo
1	60.5	70.2	71.6	<u>73.6</u>	72.1	73.2
2	48.5	<u>53.7</u>	52.9	49.4	47.5	40.7
3	30.5	38.0	36.8	<u>39.4</u>	36.7	37.9
4	74.6	<u>81.6</u>	80.6	80.9	79.7	80.2
5	40.3	<u>44.0</u>	42.7	42.3	40.1	39.1
AVG	50.9	<u>57.5</u>	56.9	57.1	55.2	54.2

TABLE II: Network prediction and pseudo-label accuracy for scene 1-5 of the ScanNet dataset. **Pred** denotes network predictions (1: pre-trained network, 2: first iteration adapted network, 3: second iteration adapted network). **Pseudo** denotes pseudo-label. Underlined numbers indicate the best performing pseudo-labels; bold numbers the best performing network.

these. We hypothesized that iterative adaptation by consecutively transforming between data representations from 2D to 3D could increase the performance further given that the labels used to generate the 3D map are more accurate. We report the accuracy achieved for each of the five adaption scenes. The pseudo-label generation and network training is performed strictly following the procedure elaborated in Section IV for all iterations. As shown in Table II, after the first adaptation step the network accuracy does not improve for four of the five scenes tested. We reason that after the first iteration the adapted network already aligns with the multi-view consistency constraint. Therefore, remapping the multi-view consistent labels into 3D cannot resolve disagreeing semantic estimations and potentially introduces discretization artifacts. This leads us to the conclusion that a single iteration of mapping and continual learning is the most effective for achieving a positive network adaptation.

D. Deployment on Handheld Device

To test our proposed method in the wild, we capture data of multiple scenes with a hand-held Azure Kinect RGB-D sensor in different office spaces. The network pre-trained on ScanNet is used to estimate an initial semantic segmentation of the captured data. We use the open-source RGB-D SLAM system ORB-SLAM2 [36] to retrieve the camera poses after bundle-adjustment and loop closures. We then build the volumetric map using these poses.

The Azure Kinect sensor cannot measure depth for reflective and light-absorbing surfaces and is limited to a maximum distance of 5.45 m. Figure 1 shows examples of the resulting pre-training, pseudo-label and adapted network predictions. As clear from the top row, the pre-trained network misclassifies multiple objects (*table*, *floor*). This evidence is in line with the significant distribution mismatch between the recorded data and the pre-training dataset, which does not include scenes with conference rooms and was recorded with a different sensor given the good supervision signal available. The generated pseudo-labels (1-Pseudo) correctly classify the *desk* in all frames. The estimated segmented map of the conference room is shown in Figure 6. Given the light-absorbing



Fig. 6: Resulting mesh in the pseudo-label generation of the lab data conference room scene.

carpet and reflective television, no depth measurement can be integrated into the volumetric map, leading to a semi-dense mapping, which induces undefined semantics when ray tracing the pseudo-labels. When training the network, we default to the 1-Pred predictions for these pixels with undefined semantics in the pseudo-labels 1-Pseudo. This allows effectively avoiding training on a sparse supervision signal, which would lead the network to wrongly classify not mapped regions (*floor*, *television*) with the label of the closest mapped pixels.

We conclude that our method generalizes well to this less controlled deployment scenario, showing the suitability of our approach for real-world robotic applications.

VI. CONCLUSION

We showed that leveraging complementary 2D-3D data representations creates a useful learning signal for semantic segmentation without any external supervision. To the best of our knowledge, we are the first to apply a continual learning strategy to adapt a multi-class semantic segmentation network in a robotic mission scenario. Our experiments show that a 3D data representation that intrinsically enforces multi-view consistency can be effectively used to retrain a network to comply with this consistency constraint already within one iteration. When evaluated on a real-world indoor dataset, our method increases the semantic segmentation performance on average by 11.8% relative to the pre-trained network. Further experiments with hand-held sensor recordings show the fitness of our proposed approach for real-world deployment. In conclusion, we show a ready-to-deploy domain adaptation approach for semantic segmentation that does not require any prior knowledge of the scene or any external supervision and can simultaneously retain knowledge of previously seen environments.

Our approach requires volumetric mapping, which is so far limited by static world assumptions and operating characteristics of existing RGB-D sensors. Further, consistent misclassifications within a scene cannot be resolved by multi-view consistency. Future work may extend our approach by including prior knowledge, e.g, identification of object instances or application of scene understanding methods potentially resolving more misclassifications. Based on our work, further research can be conducted mitigating the gap between fundamental continual learning research and real-world robotic applications, such as adaptation to multiple scenes.

REFERENCES

- [1] A. Garcia-Garcia, S. Orts-Escolano, S. Oprea, V. Villena-Martinez, and J. García Rodríguez, “A Review on Deep Learning Techniques Applied to Semantic Segmentation,” *CoRR*, vol. abs/1704.06857, 2017. [Online]. Available: <http://arxiv.org/abs/1704.06857>
- [2] M. Grinvald, F. Furrer, T. Novkovic, J. J. Chung, C. Cadena, R. Siegwart, and J. Nieto, “Volumetric Instance-Aware Semantic Mapping and 3D Object Discovery,” *IEEE Robotics and Automation Letters*, vol. 4, no. 3, pp. 3037–3044, July 2019.
- [3] A. Rosinol, M. Abate, Y. Chang, and L. Carlone, “Kimera: an Open-Source Library for Real-Time Metric-Semantic Localization and Mapping,” in *IEEE Intl. Conf. on Robotics and Automation (ICRA)*, 2020. [Online]. Available: <https://github.com/MIT-SPARK/Kimera>
- [4] A. Dai, M. Nießner, M. Zollöfer, S. Izadi, and C. Theobalt, “BundleFusion: Real-time Globally Consistent 3D Reconstruction using On-the-fly Surface Re-integration,” *ACM Transactions on Graphics 2017 (TOG)*, 2017.
- [5] P. Buzzega, M. Boschini, A. Porrello, and S. Calderara, “Rethinking Experience Replay: a Bag of Tricks for Continual Learning,” *CoRR*, vol. abs/2010.05595, 2020. [Online]. Available: <https://arxiv.org/abs/2010.05595>
- [6] A. Dai, A. X. Chang, M. Savva, M. Halber, T. Funkhouser, and M. Nießner, “ScanNet: Richly-annotated 3D Reconstructions of Indoor Scenes,” in *Proc. Computer Vision and Pattern Recognition (CVPR)*, IEEE, 2017.
- [7] J. McCormac, A. Handa, A. J. Davison, and S. Leutenegger, “SemanticFusion: Dense 3D Semantic Mapping with Convolutional Neural Networks,” *CoRR*, vol. abs/1609.05130, 2016. [Online]. Available: <http://arxiv.org/abs/1609.05130>
- [8] I. Armeni, Z. He, J. Gwak, A. Roshan Zamir, M. Fischer, J. Malik, and S. Savarese, “3D Scene Graph: A Structure for Unified Semantics, 3D Space, and Camera,” *CoRR*, vol. abs/1910.02527, 2019. [Online]. Available: <http://arxiv.org/abs/1910.02527>
- [9] A. Kolesnikov, X. Zhai, and L. Beyer, “Revisiting Self-Supervised Visual Representation Learning,” in *Proceedings of the IEEE/CVF Conference on Computer Vision and Pattern Recognition (CVPR)*, June 2019.
- [10] M. Caron, P. Bojanowski, J. Mairal, and A. Joulin, “Unsupervised Pre-Training of Image Features on Non-Curated Data,” in *Proceedings of the IEEE/CVF International Conference on Computer Vision (ICCV)*, October 2019.
- [11] J. Hou, S. Xie, B. Graham, A. Dai, and M. Nießner, “Pri3D: Can 3D Priors Help 2D Representation Learning?” *CoRR*, vol. abs/2104.11225, 2021. [Online]. Available: <https://arxiv.org/abs/2104.11225>
- [12] T. Lesort, V. Lomonaco, A. Stoian, D. Maltoni, D. Filliat, and N. Díaz-Rodríguez, “Continual Learning for Robotics: Definition, Framework, Learning Strategies, Opportunities and Challenges,” *Information Fusion*, vol. 58, pp. 52–68, 2020.
- [13] M. McCloskey and N. J. Cohen, “Catastrophic Interference in Connectionist Networks: The Sequential Learning Problem,” ser. *Psychology of Learning and Motivation*, G. H. Bower, Ed. Academic Press, 1989, vol. 24, pp. 109–165. [Online]. Available: <https://www.sciencedirect.com/science/article/pii/S0079742108605368>
- [14] D. Rolnick, A. Ahuja, J. Schwarz, T. P. Lillicrap, and G. Wayne, “Experience replay for continual learning,” *arXiv preprint arXiv:1811.11682*, 2018.
- [15] A. Chaudhry, M. Ranzato, M. Rohrbach, and M. Elhoseiny, “Efficient Lifelong Learning with A-GEM,” *CoRR*, vol. abs/1812.00420, 2018. [Online]. Available: <http://arxiv.org/abs/1812.00420>
- [16] M. Farajtabar, N. Azizan, A. Mott, and A. Li, “Orthogonal Gradient Descent for Continual Learning,” *CoRR*, vol. abs/1910.07104, 2019. [Online]. Available: <http://arxiv.org/abs/1910.07104>
- [17] A. Prabhu, P. H. Torr, and P. K. Dokania, “GDumb: A Simple Approach that Questions Our Progress in Continual Learning,” 2020.
- [18] J. Knoblauch, H. Husain, and T. Diethe, “Optimal Continual Learning has Perfect Memory and is NP-hard,” 2020.
- [19] I. J. Goodfellow, M. Mirza, D. Xiao, A. Courville, and Y. Bengio, “An Empirical Investigation of Catastrophic Forgetting in Gradient-Based Neural Networks,” 2015.
- [20] S.-A. Rebuffi, A. Kolesnikov, G. Sperl, and C. H. Lampert, “iCaRL: Incremental Classifier and Representation Learning,” 2017.
- [21] V. Lomonaco and D. Maltoni, “CORe50: a New Dataset and Benchmark for Continuous Object Recognition,” in *Proceedings of the 1st Annual Conference on Robot Learning*, ser. *Proceedings of Machine Learning Research*, S. Levine, V. Vanhoucke, and K. Goldberg, Eds., vol. 78. PMLR, 13–15 Nov 2017, pp. 17–26. [Online]. Available: <https://proceedings.mlr.press/v78/lomonaco17a.html>
- [22] U. Michieli and P. Zanuttigh, “Continual Semantic Segmentation via Repulsion-Attraction of Sparse and Disentangled Latent Representations,” *CoRR*, vol. abs/2103.06342, 2021. [Online]. Available: <https://arxiv.org/abs/2103.06342>
- [23] L. Yu, X. Liu, and J. van de Weijer, “Self-Training for Class-Incremental Semantic Segmentation,” *CoRR*, vol. abs/2012.03362, 2020. [Online]. Available: <https://arxiv.org/abs/2012.03362>
- [24] F. Cermelli, M. Mancini, S. Rota Bulò, E. Ricci, and B. Caputo, “Modeling the Background for Incremental Learning in Semantic Segmentation,” *CoRR*, vol. abs/2002.00718, 2020. [Online]. Available: <https://arxiv.org/abs/2002.00718>
- [25] A. Douillard, Y. Chen, A. Dapogny, and M. Cord, “Tackling Catastrophic Forgetting and Background Shift in Continual Semantic Segmentation,” *CoRR*, vol. abs/2106.15287, 2021. [Online]. Available: <https://arxiv.org/abs/2106.15287>
- [26] —, “PLOP: Learning without Forgetting for Continual Semantic Segmentation,” *CoRR*, vol. abs/2011.11390, 2020. [Online]. Available: <https://arxiv.org/abs/2011.11390>
- [27] H. Blum, F. Milano, R. Zurbrügg, R. Siegwart, C. Cadena, and A. Gawel, “Self-Improving Semantic Perception on a Construction Robot,” *CoRR*, vol. abs/2105.01595, 2021. [Online]. Available: <https://arxiv.org/abs/2105.01595>
- [28] H. Oleynikova, Z. Taylor, M. Fehr, R. Siegwart, and J. Nieto, “Voxblox: Incremental 3D Euclidean Signed Distance Fields for On-Board MAV Planning,” in *IEEE/RSJ International Conference on Intelligent Robots and Systems (IROS)*, 2017.
- [29] W. E. Lorensen and H. E. Cline, “Marching Cubes: A High Resolution 3D Surface Construction Algorithm,” *SIGGRAPH Comput. Graph.*, vol. 21, no. 4, p. 163–169, Aug. 1987. [Online]. Available: <https://doi.org/10.1145/37402.37422>
- [30] S. Ruder, “An overview of gradient descent optimization algorithms,” *CoRR*, vol. abs/1609.04747, 2016. [Online]. Available: <http://arxiv.org/abs/1609.04747>
- [31] R. P. K. Poudel, S. Liwicki, and R. Cipolla, “Fast-SCNN: Fast Semantic Segmentation Network,” *CoRR*, vol. abs/1902.04502, 2019. [Online]. Available: <http://arxiv.org/abs/1902.04502>
- [32] N. Silberman, D. Hoiem, P. Kohli, and R. Fergus, “Indoor Segmentation and Support Inference from RGBD Images,” in *European Conference on Computer Vision (ECCV)*, 2012.
- [33] D. P. Kingma and J. Ba, “Adam: A Method for Stochastic Optimization,” 2014, cite arxiv:1412.6980Comment: Published as a conference paper at the 3rd International Conference for Learning Representations, San Diego, 2015. [Online]. Available: <http://arxiv.org/abs/1412.6980>
- [34] S. Woop, L. Feng, I. Wald, and C. Benthin, “Embree Ray Tracing Kernels for CPUs and the Xeon Phi Architecture,” in *ACM SIGGRAPH 2013 Talks*, ser. SIGGRAPH ’13. New York, NY, USA: Association for Computing Machinery, 2013. [Online]. Available: <https://doi.org/10.1145/2504459.2504515>
- [35] L. N. Smith and N. Topin, “Super-Convergence: Very Fast Training of Residual Networks Using Large Learning Rates,” *CoRR*, vol. abs/1708.07120, 2017. [Online]. Available: <http://arxiv.org/abs/1708.07120>
- [36] R. Mur-Artal and J. D. Tardós, “ORB-SLAM2: an Open-Source SLAM System for Monocular, Stereo and RGB-D Cameras,” *CoRR*, vol. abs/1610.06475, 2016. [Online]. Available: <http://arxiv.org/abs/1610.06475>